nature geoscience

LETTERS

PUBLISHED ONLINE: 7 AUGUST 2011 | DOI: 10.1038/NGEO1218

Ice speed of a calving glacier modulated by small fluctuations in basal water pressure

Shin Sugiyama[1]*, Pedro Skvarca[2], Nozomu Naito[3], Hiroyuki Enomoto[4], Shun Tsutaki[1,5], Kenta Tone[1,5], Sebastián Marinsek[2] and Masamu Aniya[6]

Ice flow acceleration has played a crucial role in the rapid retreat of calving glaciers in Alaska[1,2], Greenland and Antarctica[3,4]. Glaciers that calve in water flow much faster than those that terminate on land, as a result of enhanced basal ice motion where basal water pressure is high[5]. However, a scarcity of subglacial observations in calving glaciers limits a mechanistic understanding. Here we present high-frequency measurements of ice speed and basal water pressures from Glaciar Perito Moreno, a fast-flowing calving glacier in Patagonia. We measured water pressure in boreholes drilled at a site where the glacier is 515 ± 5 m thick, and where more than 60% of the ice is below the level of proglacial lakes. We found that the mean basal water pressure was about 95% of the pressure imposed by the weight of the overlying ice. Moreover, changes in basal water pressure by a few per cent drove nearly 40% of the variations in ice flow speed. The ice speed was strongly correlated to air temperature, suggesting that glacier motion was modulated by water pressure changes as meltwater entered the system. We conclude that basal water pressure in calving glaciers is important for glacier dynamics, and closely connected to climate conditions.

Acceleration of fast-flowing calving glaciers is the focus of attention as it is responsible for the rapid retreat of large tidewater glaciers in Alaska[1,2] as well as the recent wastage of the Greenland and Antarctic ice sheets[3,4]. Calving glaciers flow much faster than those terminating on land as a result of basal ice motion enhanced by high basal water pressure[5]. A commonly used basal flow law states

$$u_b = k\frac{\tau_b{}^p}{(P_i - P_w)^q} = k\frac{\tau_b{}^p}{P_e{}^q} \quad (1)$$

where u_b is the basal ice speed, τ_b is the basal shear stress, P_i and P_w are ice overburden and basal water pressures, and k, p and q are empirical parameters[6,7]. As τ_b is primarily controlled by ice thickness and surface slope, changes in basal water pressure play a critical role in short-term ice speed variations. Observations in mountain glaciers have shown rapid acceleration as basal water pressure approaches ice overburden pressure[8–10], which confirms the nonlinear dependence of the basal ice speed on the effective pressure defined by $P_e = P_i - P_w$. The hydraulic head within a calving glacier is expected to be higher than the surface level of the proglacial water body, which maintains basal water pressure closer to ice overburden. According to the inverse proportionality of u_b to P_e, small perturbations in P_w near P_i result in large ice speed variations. Moreover, changes in P_i due to glacier thinning or thickening have a great impact on the ice speed as well. These characteristics make calving glacier dynamics more susceptible to external forcing than land terminating glaciers. Studying the response of ice speed to the changes in P_e is thus crucial for predicting the future evolution of calving glaciers. However, only a very few water pressure measurements have been performed in calving glaciers and have never been reported in Patagonia.

The Patagonia Icefields cover an area of 1.70×10^4 km^2 (refs 11, 12), forming the second largest ice mass in the southern hemisphere.

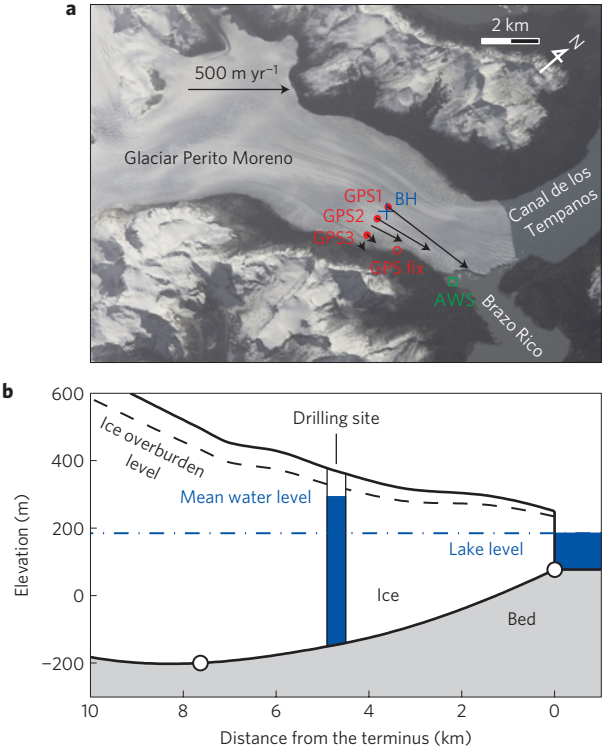

Figure 1 | Satellite image and longitudinal cross section of Glaciar Perito Moreno. a, GPS (filled circle, open circle), drilling (plus) and air temperature measurement (box) sites are indicated with ice flow vectors measured from 31 December 2008 to 7 January 2009. The image was taken on 27 March 2002 (image courtesy of the Image Science and Analysis Laboratory, NASA Johnson Space Center). **b**, The bed profile is drawn by interpolation of observational data points (open circle[16]). Mean borehole water level during the measurement period is indicated.

[1]Institute of Low Temperature Science, Hokkaido University, Nishi8, Kita19, Sapporo, Japan, [2]Instituto Antártico Argentino, Cerrito 1248, C1010AAZ Buenos Aires, Argentina, [3]Hiroshima Institute of Technology, 2-1-1 Miyake, Saeki-ku, Hiroshima, Japan, [4]National Insitute of Polar Research, 10-3 Midori-cho, Tachikawa, Japan, [5]Graduate School of Environmental Science, Hokkaido University, Nishi5, Kita10, Sapporo, Japan, [6]University of Tsukuba, 1-1-1 Tennodai, Tsukuba, Japan. *e-mail: sugishin@lowtem.hokudai.ac.jp.

© 2011 Macmillan Publishers Limited. All rights reserved.

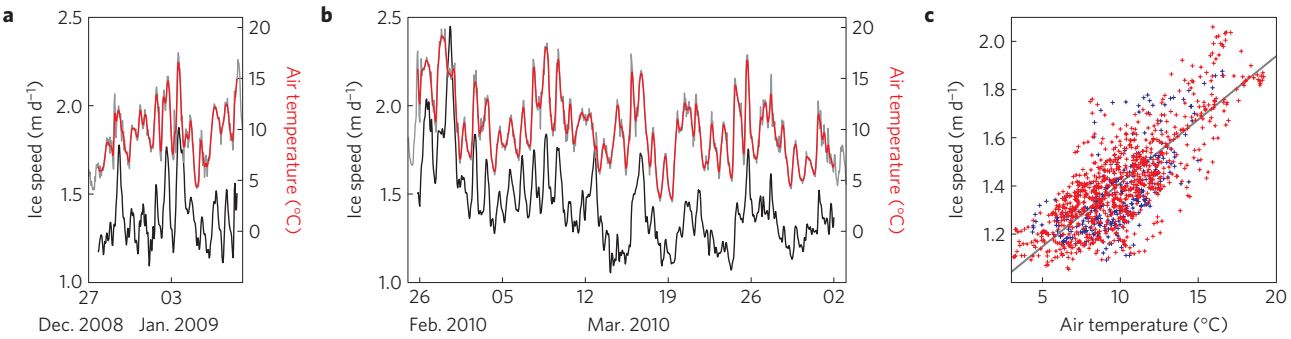

Figure 2 | Ice speed and air temperature measured in 2008/09 and 2010 austral summer seasons. a,b, Ice speed at GPS1 (black) and air temperature (red) obtained by filtering hourly data (grey). **c**, Scatter plot of hourly ice speed and air temperature for the measurements in 2008/09 (blue) and 2010 (red).

Most of the glaciers in Patagonia have been retreating and thinning for the past several decades[12,13], which contributes to a sea-level rise of $0.042–0.105 \pm 0.011$ mm yr^{-1} (ref. 14). Warming climate is a likely cause of the ice loss[13], but changes in glacier dynamics is important, as more than 80% of major outlet glaciers discharge ice into lakes and the ocean by calving[14,15]. Glaciar Perito Moreno (GPM) is one such glacier, with a length of 30 km and an area of 258 km^2, situated in the southeast of the Southern Patagonia Icefield[13]. In the region extending 8 km from the terminus, approximately 50–70% of ice thickness is below the surface of proglacial lakes, Brazo Rico and Canal de los Témpanos (Fig. 1; ref. 16). In this region, ice speed is more than 400 m yr^{-1} and the glacier is 200–800 m thick along the central flowline[16].

In the austral summer 2008/09 and 2010, we operated three GPS (Global Positioning System) receivers on GPM at hourly intervals to measure short-term ice speed variations and their relationship with air temperature and basal water pressure. The study site was 4.7 km from the terminus and the bed elevation was more than 380 m below the lake level[16] (Fig. 1). In March 2010, we drilled two boreholes with a hot-water drilling technique at 160 m south of GPS1 (ref. 17; Fig. 1a). According to the length of the hose used for the drilling, ice thickness was 515 ± 5 m. The water level in the boreholes dropped before the drill reached the bed, which occurred at depths of 176 and 344 m for the first drilling and at 375 m for the second drilling. After the drilling, the water level was measured every 10–30 min using pressure sensors suspended in the boreholes. Details of the measurements are described in the Methods section.

Ice speed showed diurnal and longer-term variations over the observation periods (Fig. 2a,b). During the one-month measurement period in 2010, ice speed varied by +71 to −26% from the mean of 1.43 m d^{-1}. An intriguing feature is the strong correlation between the ice speed and air temperature. Hourly ice speed correlated positively to the air temperature, with a correlation coefficient $r = 0.76$ for the entire observation period (Fig. 2c and Supplementary Table S1). A maximum correlation was achieved when the ice speed lag was 1 h relative to the temperature (Supplementary Fig. S1). Linear regression indicates that the ice speed deviated ± 0.053 m d^{-1} for a temperature change of ± 1 °C. A likely mechanism of the air-temperature-dependent ice speed variation was the change in basal water pressure driven by meltwater input. Melt production is commonly related to the positive degree day (ref. 18) as we observed at GPM (Supplementary Fig. S2).

From 4 to 13 March 2010, mean water levels in the boreholes were 440 (BH1) and 450 m (BH1) above the bed, that is, 110–120 m higher than the proglacial lake level (Figs 1b and 3a). This observation indicated that the basal water pressure was at 94–96% of the ice overburden pressure and the effective pressure was only 190–280 kPa. The water level oscillated in a diurnal manner with an amplitude of 10–15 m from 5 to 10 March (Fig. 3a). The levels were not exactly the same in the two boreholes, but the oscillations were in phase. The ice speed at GPS1 and GPS2 was correlated to the water level (Fig. 3a–c). The range of the ice speed variation was 37% of the mean at GPS1, whereas that of the water level was only 4–6% (Fig. 3c).

The borehole data show that the glacier bed is exposed to consistently high water pressure, and large diurnal ice speed variations are driven by small pressure fluctuations near the ice overburden. These observations are consistent with equation (1), which relates the basal ice speed to the inverse power of effective pressure. A numerical ice flow model shows that 94% of the observed ice speed at GPS1 is due to basal ice motion (Supplementary Fig. S3). Thus, we neglected the contribution of internal ice deformation to the total glacier motion, and performed the fitting of equation (1) to the ice speed (GPS1) and pressure (mean of BH1 and BH2) data to find the dependence of basal ice speed on the effective pressure. The least square fitting yields

$$u_b = 0.91 P_e^{-0.35} \quad \sigma = 0.061 \qquad (2)$$

where u_b and the root mean square error σ are in m d^{-1} and P_e is in MPa (Supplementary Table S2). The fitting curve clearly indicates that the basal ice speed of GPM is highly dependent on the effective pressure within the observed pressure range (Fig. 3d).

Water pressure beneath a calving glacier was previously measured at Columbia Glacier, an Alaskan tidewater glacier with dimensions similar to those of GPM (about 5 km wide and 400–1,000 m thick). Basal water pressure was consistently high and the effective pressure varied within a range between −100 and 300 kPa (ref. 19). These figures are similar to those we observed at GPM, but ice speed at Columbia Glacier was not well correlated with water pressure nor with air temperature. It was argued that basal pressure was non-uniformly distributed and the borehole measurements did not represent spatially averaged pressure, which is more important for ice speed variations[20]. It is assumed that horizontal patterns of subglacial hydraulic conditions at Columbia Glacier are less uniform than those at GPM, as described below.

Our observation revealed a clear relationship between air temperature and ice speed, which implies that basal water pressure is controlled primarily by the meltwater production rate. However, previous studies showed that basal pressure is not simply a function of water input, but that it is substantially influenced by the evolution of subglacial drainage conditions over a timescale of days to months[10,21]. For example, a melt event in the early ablation season elevates basal pressure, resulting in a speed-up event[22,23]. The speed-up ceases as a drainage system develops and water drains downglacier more efficiently. Moreover, the response of basal pressure to surface melt is often delayed more than several

© 2011 Macmillan Publishers Limited. All rights reserved.

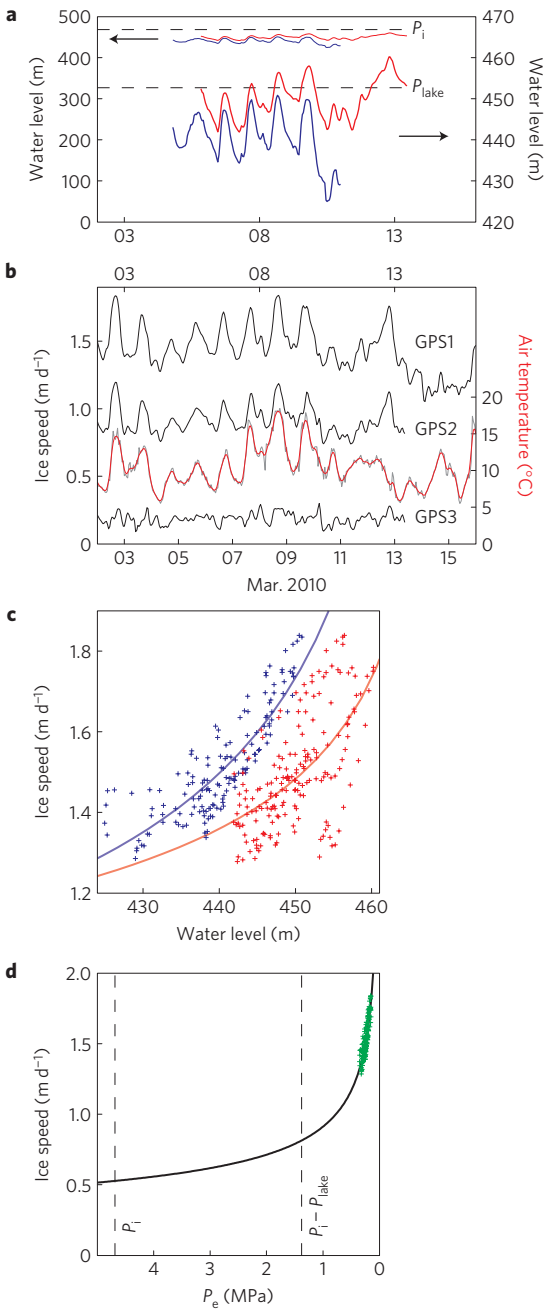

Figure 3 | Ice speed and borehole water levels. a, Water levels relative to the bed in BH1 (blue) and BH2 (red) for two different scales. Dashed lines indicate ice overburden (P_i) and lake levels (P_{lake}) in the left axis. **b**, Ice speed at GPS1–3 (black) and air temperature (red). **c**, Hourly ice speed at GPS1 versus water level in BH1 (blue) and BH2 (red) with curves obtained by fitting equation (1) to the data (Supplementary Table S2). **d**, Ice speed versus effective pressure with a fitting curve that represents equation (2). Dashed lines indicate the effective pressures for water levels equal to zero ($P_e = P_i$) and to the lake surface ($P_e = P_i - P_{lake}$).

hours[10]. At GPM, the consistently high correlation between the ice speed and the air temperature suggests a swift transfer of surface meltwater to the basal hydraulic system and a relatively constant drainage efficiency. Presumably, the meltwater immediately drains into crevasses which cover the greater part of the glacier, and it reaches the hydraulic system within a short time, as the hydraulic head is only 60–80 m below the surface. High water pressure and a large amount of meltwater input all year round[16] are favourable conditions for maintaining the drainage systems in a more uniform way as compared with other glaciers. Spatially uniform drainage system configurations are suggested by other observations: the englacial drainage of the borehole water during the drilling, very similar water level variations in the two boreholes and synchronous ice speed variations at GPS1 and GPS2. These observations contrast to those reported for other glaciers, which suggested non-uniformly distributed subglacial hydraulic conditions[24,25].

The observations in GPM have important implications for studying the dynamic behaviour of calving glaciers. First, the borehole levels were significantly higher than the lake level, which disagrees with a common assumption that equates the subglacial hydraulic head to the surface of the proglacial water body[26]. This is crucial, as the ice speed is greatly underestimated with such an assumption. Second, we confirmed that the calving glacier dynamics are very sensitive to small basal water pressure variations near the ice overburden. Together with the close correlation of the ice speed with the air temperature, calving glaciers are assumed to be very susceptible to changing climate. If the ice speed increases under the rising air temperature condition, ice dissipation by calving increases, causing thinning of the glacier. The thinning in turn reduces the effective pressure, which results in further acceleration of the glacier[5,27]. According to equation (1), basal ice speed in GPM is negatively correlated with ice thickness under the observed basal water pressure conditions (Supplementary Fig. S4).

Recent studies using numerical models reproduced several aspects of the dynamic behaviour of outlet glaciers in Greenland by capturing calving processes[28]. However, basal water pressure is not well imposed in the model as described above. The foregoing discussion suggests a positive feedback effect between thinning and acceleration of calving glaciers, which can be captured by modelling only with realistic basal water pressure and an effective pressure dependent basal flow law. Further investigations of subglacial processes and the accurate treatment of basal conditions in a model are thus crucial for predicting the future evolution of calving glaciers in Patagonia and Alaska, as well as marine-terminating outlet glaciers in Greenland and Antarctica.

Methods

Ice speed was measured at GPS1–3 (Fig. 1a) with dual frequency GPS receivers (Leica System 1200) from 27 December 2008 to 8 January 2009 and from 25 February to 2 April 2010. We installed 2-m-long aluminium poles in the ice and mounted GPS antennae at the top of the poles. The GPS receivers were activated every hour for 30 min and the satellite signals were processed with data recorded at a reference GPS station fixed on a stable rock on a side moraine (Fig. 1a). GPS processing software (Leica Geo Office) was used to obtain stake positions with an accuracy of 3–5 mm (ref. 10). We computed horizontal ice speed after smoothing the data with a Gaussian filter having a bandwidth of 1.5 h. This bandwidth was chosen so that the mean deviation of the data from the smoothed curve was equivalent to the positioning accuracy. The relative error in the computed hourly ice speed was 7–12% for the mean speed at GPS1, and the actual error after the smoothing procedure was smaller than this estimate.

Boreholes were drilled by means of a hot-water drilling system consisting of two high-pressure hot-water machines (Kärcher HDS1000BE) at a mean drilling rate of 49 m h^{-1} (ref. 17). The weight of the drilling hose was monitored during the drilling to detect the glacier bed. The ice thickness was determined as 515 ± 5 m from the length of the hose used for the drilling and its extension due to its own weight. Water levels in the boreholes BH1 and BH2 were measured with water pressure sensors (Geokon 4500S and HOBO U20-001-03) installed at 98 ± 1 and 120 ± 0.1 m from the surface, respectively. The measurement ranges/accuracies of the sensors were -0.1–2 MPa/± 200 mm (BH1) and 0–0.85 MPa/± 38 mm (BH2). The pressure data were corrected for atmospheric pressure recorded every hour at the air temperature measurement site. The data availability was limited to 4–12 March at BH1, as the borehole was isolated from the subglacial drainage network afterwards, and 5–13 March at BH2, as we could not retrieve the data after the sensor got stuck in the borehole.

Air temperature was measured near the glacier front at the shore of Brazo Rico (Fig. 1a). A temperature sensor (Vaisala, HMP35AC) protected with a non-aspirated radiation shield was installed on a mast at 2 m above the rock surface. The temperature was measured every 10 s with an accuracy of ± 0.4 °C to record hourly mean values in a datalogger (Campbell, 21X; ref. 29).

© 2011 Macmillan Publishers Limited. All rights reserved.

Received 15 March 2011; accepted 28 June 2011; published online 7 August 2011

References

1. Krimmel, R. M. Photogrammetric data set, 1957–2000, and bathymetric measurements for Columbia Glacier, Alaska. *US Geol. Surv. Wat. Resour. Invest. Rep.* 01–4089 (2001).
2. O'Neel, S., Echelmeyer, K. A. & Motyka, R. J. Short-term flow dynamics of a retreating tidewater glacier: LeConte Glacier, Alaska, USA. *J. Glaciol.* **47,** 567–578 (2001).
3. Rignot, E. & Kanagaratnam, P. Changes in the velocity structure of the Greenland ice sheet. *Science* **311,** 986–990 (2006).
4. Pritchard, H. D., Arthern, R. J., Vaughan, D. G. & Edwards, L. A. Extensive dynamic thinning on the margins of the Greenland and Antarctic ice sheets. *Nature* **461,** 971–975 (2009).
5. Meier, M. F. & Post, A. Fast tidewater glaciers. *J. Geophys. Res.* **92,** 9051–9058 (1987).
6. Greve, R. & Blatter, H. *Dynamics of Ice Sheets and Glaciers* (Springer, 2009).
7. Bindschadler, R. The importance of pressurized subglacial water in separation and sliding at the glacier bed. *J. Glaciol.* **47,** 3–19 (1983).
8. Iken, A. & Bindschadler, R. A. Combined measurements of subglacial water pressure and surface velocity of Findelengletscher, Switzerland: Conclusions about drainage system and sliding mechanism. *J. Glaciol.* **32,** 28–47 (1986).
9. Jansson, P. Water pressure and basal sliding on Storglaciären, northern Sweden. *J. Glaciol.* **41,** 232–240 (1995).
10. Sugiyama, S. & Gudmundsson, G. H. Short-term variations in glacier flow controlled by subglacial water pressure at Lauteraargletscher, Bernese Alps, Switzerland. *J. Glaciol.* **50,** 353–362 (2004).
11. Aniya, M., Naruse, R., Shizukuishi, M., Skvarca, P. & Casassa, G. Monitoring recent glacier variations in the Southern Patagonia Icefield, utilizing remote sensing data. *Int. Arch. Photogram. Rem. Sens.* **29,** 87–94 (1992).
12. Rivera, A., Benham, T., Casassa, G., Bamber, J. & Dowdeswell, J. A. Ice elevation and areal changes of glaciers from the Northern Patagonia Icefield, Chile. *Glob. Planet. Change* **59,** 126–137 (2007).
13. Aniya, M., Sato, H., Naruse, R., Skvarca, P. & Casassa, G. Recent glacier variations in the Southern Patagonia Icefield, South America. *Arct. Alp. Res.* **29,** 1–12 (1997).
14. Rignot, E., Rivera, A. & Casassa, G. Contribution of the Patagonia Icefields of South America to sea level rise. *Science* **302,** 434–437 (2003).
15. Warren, C. R. & Aniya, M. The calving glaciers of southern South America. *Glob. Planet. Change* **22,** 59–77 (1999).
16. Stuefer, M., Rott, H. & Skvarca, P. Glaciar Perito Moreno, Patagonia: Climate sensitivities and glacier characteristics preceding the 2003/04 and 2005/06 damming events. *J. Glaciol.* **53,** 3–16 (2007).
17. Sugiyama, S. *et al.* Hot-water drilling at Glaciar Perito Moreno, Southern Patagonia Icefield. *Bull. Glaciol. Res.* **28,** 27–32 (2010).
18. Ohmura, A. Physical basis for the temperature-based melt-index method. *J. Appl. Meteorol.* **40,** 753–761 (2001).
19. Meier, M. F. *et al.* Mechanical and hydrologic basis for the rapid motion of a large tidewater glacier: 1. Observations. *J. Geophys. Res.* **99,** 15219–15229 (1994).
20. Kamb, B. *et al.* Mechanical and hydrologic basis for the rapid motion of a large tidewater glacier: 2. Interpretation. *J. Geophys. Res.* **99,** 15231–15244 (1994).
21. Gordon, S. *et al.* Seasonal reorganization of subglacial drainage inferred from measurements in boreholes. *Hydrol. Processes* **12,** 105–133 (1998).
22. Iken, A., Röthlisberger, H., Flotron, A. & Haeberli, W. The uplift of Unteraargletscher at the beginning of the melt season—a consequence of water storage at the bed? *J. Glaciol.* **29,** 28–47 (2001).
23. Mair, D., Nienow, P., Willis, I. & Sharp, M. Spatial patterns of glacier motion during a high-velocity event: Haut Glacier d'Arolla, Switzerland. *J. Glaciol.* **47,** 9–20 (2001).
24. Murray, T. & Clarke, G. K. C. Black-box modeling of the subglacial water system. *J. Geophys. Res.* **100,** 10231–10245 (1995).
25. Nienow, P. W. *et al.* Hydrological controls on diurnal ice flow variability in valley glaciers. *J. Geophys. Res.* **110,** F04002 (2005).
26. Vieli, A., Funk, M. & Blatter, H. Flow dynamics of tidewater glaciers: A numerical modelling approach. *J. Glaciol.* **47,** 595–606 (2001).
27. Pfeffer, W. T. A simple mechanism for irreversible tidewater glacier retreat. *J. Geophys. Res.* **112,** F03S25 (2007).
28. Nick, F. M., Vieli, A., Howat, I. M. & Joughin, I. Large-scale changes in Greenland outlet glacier dynamics triggered at the terminus. *Nature Geosci.* **2,** 110–114 (2009).
29. Stuefer, M. *Investigations on Mass Balance and Dynamics of Moreno Glacier Based on Field Measurements and Satellite Imagery* PhD thesis, Univ. Innsbruck (1999).

Acknowledgements

We thank the members of the field campaign at Glaciar Perito Moreno in 2008/2009 and 2010 for their help on the glacier. Hielo y Aventura S. A. offered logistic support and Gendarmeria Nacional Argentina operated helicopter transportation. Drilling equipment was constructed by the workshop of the Institute of Low Temperature Science, Hokkaido University. Thanks are extended to R. Greve and H. Blatter for comments on the manuscript. This research was funded by the Japanese Ministry of Education, Science, Sports and Culture, Grant-in-Aid 18251002 (2005–2009) and 23403006 (2011–2014).

Author contributions

S.S., P.S. and M.A. designed the research. S.S., N.N., H.E. and K.T. drilled the boreholes. S.S., P.S., N.N., S.T., K.T. and S.M. collected the water pressure and GPS data. S.S. analysed the data and wrote the manuscript. The authors discussed the results and commented jointly on the manuscript.

Additional information

The authors declare no competing financial interests. Supplementary information accompanies this paper on www.nature.com/naturegeoscience. Reprints and permissions information is available online at http://www.nature.com/reprints. Correspondence and requests for materials should be addressed to S.S.

© 2011 Macmillan Publishers Limited. All rights reserved.